the blood, accumulate in vascular wall, and contribute to vascular lesion formation [38,39]. It has also been shown that the CXC chemokine SDF-1α is a pivotal chemotactic factor of bone marrow-derived VSMC progenitor cells [40]. In the present study, the number of circulating Sca-1$^+$/c-Kit$^-$/Lin$^-$ cells (interpreted as bone marrow-derived VSMC progenitor cells) [41] and the cardiac SDF-1α protein levels were markedly increased in the 2/3NX triple NOSs$^{-/-}$ mice. Thus, it is possible that SDF-1α-induced recruitment of the circulating bone marrow-derived VSMC progenitor cells was also involved in the occurrence of acute myocardial infarction in the 2/3NX triple NOSs$^{-/-}$ mice.

Renin–angiotensin system activation (as evidenced by increases in plasma angiotensin II levels and cardiac ACE expression levels) and oxidative stress (as indicated by elevation in urinary 8-isoprostane levels) were noted in the 2/3NX triple NOSs$^{-/-}$ mice. Based on these findings, we used the selective and potent AT1 receptor blocker, irbesartan, and the antioxidant calcium channel antagonist, amlodipine, to further examine the involvement of renin–angiotensin system activation and oxidative stress in the pathogenesis of acute myocardial infarction. It has been indicated that amlodipine is a charged molecule, is highly lipophilic, and has a much higher affinity for lipid-laden cellular membranes than do other calcium channel antagonists, exerting a powerful antioxidant activity, independent of its calcium channel antagonistic action [42]. In the present study, the simultaneous treatment with irbesartan and amlodipine potently suppressed renin–angiotensin system activation and oxidative stress, and markedly prevented coronary arteriosclerotic lesion formation and the incidence of myocardial infarction, and improved the prognosis of the 2/3NX triple NOSs$^{-/-}$ mice. Furthermore, the simultaneous irbesartan/amlodipine treatment significantly ameliorated the cardiovascular risk factors, the increased number of circulating Sca-1$^+$/c-Kit$^-$/Lin$^-$ cells, and the enhanced cardiac SDF-1α expression levels in those mice. Therefore, it is conceivable that renin–angiotensin system activation and oxidative stress are involved in the pathogenesis of acute myocardial infarction in the 2/3NX triple NOSs$^{-/-}$ mice. Consistent with these results, it has been reported that renin–angiotensin system activation and oxidative stress are recognized in patients with CKD, and that both factors accelerate arteriosclerotic lesion formation [13].

The treatment with hydralazine exerted an anti-hypertensive action to the same extent as the combined treatment with irbesartan and amlodipine. However, the hydralazine treatment did not show any beneficial effects on the incidence of myocardial infarction, the prognosis, or the pro-arteriosclerotic parameters in the 2/3NX triple NOSs$^{-/-}$ mice. Thus, it is suggested that the beneficial effects of the irbesartan/amlodipine treatment are not caused by changes of blood pressure.

4.4. Clinical perspectives

The mechanism(s) by which CKD is complicated by acute myocardial infarction is not fully understood. Our findings provide novel evidence that the NO/NOSs system plays a pivotal role in the pathogenesis of this reno-cardiac connection. The AT1 receptor blockers and calcium channel antagonists are widely used to treat hypertension in patients with CKD, and the former are also employed to retard the progression of CKD. In the present study, the clinical dosage of irbesartan and amlodipine exhibited cardiovascular and renal protective actions in the 2/3NX triple NOSs$^{-/-}$ mice. These results suggest the therapeutic importance of the AT1 receptor blockers and calcium channel antagonists in preventing complications of acute myocardial infarction in CKD as well as the progression of CKD.

4.5. Conclusions

We have succeeded in developing a novel experimentally useful model of acute myocardial infarction. Renin–angiotensin system activation, oxidative stress, cardiovascular risk factors, and SDF-1α-induced recruitment of circulating bone marrow-derived VSMC progenitor cells appear to be involved in the pathogenesis of acute myocardial infarction in the 2/3NX triple NOSs$^{-/-}$ mice. This model may contribute to the elucidation of the pathogenesis of acute myocardial infarction, and to the research and development of novel therapeutic strategies for preventing this fatal cardiovascular disorder.

Sources of funding

This work was supported in part by a Grant-in-Aid for Scientific Research from the Japan Society for the Promotion of Science (23590305), Special Account Budgets for Education and Research granted by the Japan Ministry of Education, Grants from the Promotion Project of Medical Clustering of Okinawa prefecture and the University of the Ryukyus, and a Grant and Donation from the Sumitomo Dainippon Pharma Co, Japan. These funding sources had no involvement regarding the conduct of the research or preparation of the article.

Conflict of interest

We obtained irbesartan and amlodipine from the Sumitomo Dainippon Pharma Co, Japan, and received a research fund and donation from the company.

Appendix A. Supplementary data

Supplementary data to this article can be found online at http://dx.doi.org/10.1016/j.yjmcc.2014.09.021.

References

[1] White HD, Chew DP. Acute myocardial infarction. Lancet 2008;372:570–84.
[2] Antman EM. ST-segment elevation myocardial infarction: pathology, pathophysiology, and clinical features. In: Libby P, Bonow RO, Mann D, Zipes DP, editors. Braunwald's Heart Disease. 9th ed. Philadelphia: Elsevier Saunders; 2012. p. 1087–110.
[3] Antman EM, Loscaldo J. ST-segment elevation myocardial infarction. In: Longo DL, Fauci AS, Kasper DL, Hauser SL, Jameson JL, Loscalzo J, editors. Harrison's Principles of Internal Medicine. 18th ed. New York: Mc Graw Hill Medical; 2012. p. 2012–35.
[4] Bredt DS, Snyder SH. Nitric oxide: a physiological messenger molecule. Annu Rev Biochem 1994;63:175–95.
[5] Ignarro LJ. Biosynthesis and metabolism of endothelium-derived nitric oxide. Annu Rev Pharmacol Toxicol 1990;30:535–60.
[6] Moncada S, Palmer RMJ, Higgs EA. Nitric oxide: physiology, pathophysiology, and pharmacology. Pharmacol Rev 1991;43:109–42.
[7] Murad F. What are the molecular mechanisms for the antiproliferative effects of nitric oxide and cGMP in vascular smooth muscle? Circulation 1997;95:1101–3.
[8] Shimokawa H. Primary endothelial dysfunction: atherosclerosis. J Mol Cell Cardiol 1999;31:23–37.
[9] Tsutsui M, Shimokawa H, Otsuji Y, Yanagihara N. Pathophysiological relevance of NO signaling in the cardiovascular system: novel insight from mice lacking all NO synthases. Pharmacol Ther 2010;128:499–508.
[10] Morishita T, Tsutsui M, Shimokawa H, Sabanai K, Tasaki H, Suda O, et al. Nephrogenic diabetes insipidus in mice lacking all nitric oxide synthase isoforms. Proc Natl Acad Sci U S A 2005;102:10616–21.
[11] Nakata S, Tsutsui M, Shimokawa H, Suda O, Morishita T, Shibata K, et al. Spontaneous myocardial infarction in mice lacking all nitric oxide synthase isoforms. Circulation 2008;117:2211–23.
[12] Coresh J, Selvin E, Stevens LA, Manzi J, Kusek JW, Eggers P, et al. Prevalence of chronic kidney disease in the United States. JAMA 2007;298:2038–47.
[13] Lopez-Novoa JM, Martinez-Salgado C, Rodriguez-Pena AB, Lopez-Hernandez FJ. Common pathophysiological mechanisms of chronic kidney disease: therapeutic perspectives. Pharmacol Ther 2010;128:61–81.
[14] Ninomiya T, Kiyohara Y, Kubo M, Tanizaki Y, Doi Y, Okubo K, et al. Chronic kidney disease and cardiovascular disease in a general Japanese population: the Hisayama Study. Kidney Int 2005;68:228–36.
[15] Ninomiya T, Kiyohara Y, Tokuda Y, Doi Y, Arima H, Harada A, et al. Impact of kidney disease and blood pressure on the development of cardiovascular disease: an overview from the Japan Arteriosclerosis Longitudinal Study. Circulation 2008;118:2694–701.
[16] Shoji T, Abe T, Matsuo H, Egusa G, Yamasaki Y, Kashihara N, et al. Chronic kidney disease, dyslipidemia, and atherosclerosis. J Atheroscler Thromb 2012;19:299–315.
[17] Miyazaki-Anzai S, Levi M, Kratzer A, Ting TC, Lewis LB, Miyazaki M. Farnesoid X receptor activation prevents the development of vascular calcification in ApoE−/− mice with chronic kidney disease. Circ Res 2010;106:1807–17.

[18] Pelletier CC, Koppe L, Croze ML, Kalbacher E, Vella RE, Guebre-Egziabher F, et al. White adipose tissue overproduces the lipid-mobilizing factor zinc alpha2-glycoprotein in chronic kidney disease. Kidney Int 2013;83:878–86.
[19] Schober A, Knarren S, Lietz M, Lin EA, Weber C. Crucial role of stromal cell-derived factor-1alpha in neointima formation after vascular injury in apolipoprotein E-deficient mice. Circulation 2003;108:2491–7.
[20] Moreno Junior H, Nathan LP, Metze K, Costa SK, Antunes E, Hyslop S, et al. Non-specific inhibitors of nitric oxide synthase cause myocardial necrosis in the rat. Clin Exp Pharmacol Physiol 1997;24:349–52.
[21] Ono Y, Ono H, Matsuoka H, Fujimori T, Frohlich ED. Apoptosis, coronary arterial remodeling, and myocardial infarction after nitric oxide inhibition in SHR. Hypertension 1999;34:609–16.
[22] Verhagen AM, Hohbach J, Joles JA, Braam B, Boer P, Koomans HA, et al. Unchanged cardiac angiotensin II levels accompany losartan-sensitive cardiac injury due to nitric oxide synthase inhibition. Eur J Pharmacol 2000;400:239–47.
[23] Ikeda K, Nara Y, Tagami M, Yamori Y. Nitric oxide deficiency induces myocardial infarction in hypercholesterolaemic stroke-prone spontaneously hypertensive rats. Clin Exp Pharmacol Physiol 1997;24:344–8.
[24] Suda O, Tsutsui M, Morishita T, Tanimoto A, Horiuchi M, Tasaki H, et al. Long-term treatment with N(omega)-nitro-L-arginine methyl ester causes arteriosclerotic coronary lesions in endothelial nitric oxide synthase-deficient mice. Circulation 2002;106:1729–35.
[25] Braun A, Trigatti BL, Post MJ, Sato K, Simons M, Edelberg JM, et al. Loss of SR-BI expression leads to the early onset of occlusive atherosclerotic coronary artery disease, spontaneous myocardial infarctions, severe cardiac dysfunction, and premature death in apolipoprotein E-deficient mice. Circ Res 2002;90:270–6.
[26] Zhang S, Picard MH, Vasile E, Zhu Y, Raffai RL, Weisgraber KH, et al. Diet-induced occlusive coronary atherosclerosis, myocardial infarction, cardiac dysfunction, and premature death in scavenger receptor class B type I-deficient, hypomorphic apolipoprotein ER61 mice. Circulation 2005;111:3457–64.
[27] Nakagawa-Toyama Y, Zhang S, Krieger M. Dietary manipulation and social isolation alter disease progression in a murine model of coronary heart disease. PLoS One 2012;7:e47965.
[28] Taddei S, Virdis A, Ghiadoni L, Magagna A, Favilla S, Pompella A, et al. Restoration of nitric oxide availability after calcium antagonist treatment in essential hypertension. Hypertension 2001;37:943–8.
[29] Tsuji H, Venditti Jr FJ, Manders ES, Evans JC, Larson MG, Feldman CL, et al. Reduced heart rate variability and mortality risk in an elderly cohort. The Framingham Heart Study. Circulation 1994;90:878–83.
[30] Baylis C. Nitric oxide deficiency in chronic kidney disease. Am J Physiol Renal Physiol 2008;294:F1–9.
[31] Schmidt RJ, Baylis C. Total nitric oxide production is low in patients with chronic renal disease. Kidney Int 2000;58:1261–6.
[32] Wever R, Boer P, Hijmering M, Stroes E, Verhaar M, Kastelein J, et al. Nitric oxide production is reduced in patients with chronic renal failure. Arterioscler Thromb Vasc Biol 1999;19:1168–72.
[33] Lu TM, Chung MY, Lin CC, Hsu CP, Lin SJ. Asymmetric dimethylarginine and clinical outcomes in chronic kidney disease. Clin J Am Soc Nephrol 2011;6:1566–72.
[34] Piatti P, Di Mario C, Monti LD, Fragasso G, Sgura F, Caumo A, et al. Association of insulin resistance, hyperleptinemia, and impaired nitric oxide release with in-stent restenosis in patients undergoing coronary stenting. Circulation 2003;108:2074–81.
[35] Cooke JP. ADMA: its role in vascular disease. Vasc Med 2005;10(Suppl. 1):S11–7.
[36] Cook S. Coronary artery disease, nitric oxide and oxidative stress: the "Yin-Yang" effect, a Chinese concept for a worldwide pandemic. Swiss Med Wkly 2006;136:103–13.
[37] Shamseddin MK, Parfrey PS. Sudden cardiac death in chronic kidney disease: epidemiology and prevention. Nat Rev Nephrol 2011;7:145–54.
[38] Sata M, Saiura A, Kunisato A, Tojo A, Okada S, Tokuhisa T, et al. Hematopoietic stem cells differentiate into vascular cells that participate in the pathogenesis of atherosclerosis. Nat Med 2002;8:403–9.
[39] Shimizu K, Sugiyama S, Aikawa M, Fukumoto Y, Rabkin E, Libby P, et al. Host bone-marrow cells are a source of donor intimal smooth- muscle-like cells in murine aortic transplant arteriopathy. Nat Med 2001;7:738–41.
[40] Ceradini DJ, Kulkarni AR, Callaghan MJ, Tepper OM, Bastidas N, Kleinman ME, et al. Progenitor cell trafficking is regulated by hypoxic gradients through HIF-1 induction of SDF-1. Nat Med 2004;10:858–64.
[41] Zhang LN, Wilson DW, da Cunha V, Sullivan ME, Vergona R, Rutledge JC, et al. Endothelial NO synthase deficiency promotes smooth muscle progenitor cells in association with upregulation of stromal cell-derived factor-1alpha in a mouse model of carotid artery ligation. Arterioscler Thromb Vasc Biol 2006;26:765–72.
[42] Mason RP, Walter MF, Trumbore MW, Olmstead Jr EG, Mason PE. Membrane antioxidant effects of the charged dihydropyridine calcium antagonist amlodipine. J Mol Cell Cardiol 1999;31:275–81.

Neurosteroids Allopregnanolone Sulfate and Pregnanolone Sulfate Have Diverse Effect on the α Subunit of the Neuronal Voltage-gated Sodium Channels $Na_v1.2$, $Na_v1.6$, $Na_v1.7$, and $Na_v1.8$ Expressed in *Xenopus* Oocytes

Takafumi Horishita, M.D., Ph.D., Nobuyuki Yanagihara, Ph.D., Susumu Ueno, M.D., Ph.D., Yuka Sudo, Ph.D., Yasuhito Uezono, M.D., Ph.D., Dan Okura, M.D., Tomoko Minami, M.D., Takashi Kawasaki, M.D., Ph.D., Takeyoshi Sata, M.D., Ph.D.

ABSTRACT

Background: The neurosteroids allopregnanolone and pregnanolone are potent positive modulators of γ-aminobutyric acid type A receptors. Antinociceptive effects of allopregnanolone have attracted much attention because recent reports have indicated the potential of allopregnanolone as a therapeutic agent for refractory pain. However, the analgesic mechanisms of allopregnanolone are still unclear. Voltage-gated sodium channels (Na_v) are thought to play important roles in inflammatory and neuropathic pain, but there have been few investigations on the effects of allopregnanolone on sodium channels.

Methods: Using voltage-clamp techniques, the effects of allopregnanolone sulfate (APAS) and pregnanolone sulfate (PAS) on sodium current were examined in *Xenopus* oocytes expressing $Na_v1.2$, $Na_v1.6$, $Na_v1.7$, and $Na_v1.8$ α subunits.

Results: APAS suppressed sodium currents of $Na_v1.2$, $Na_v1.6$, and $Na_v1.7$ at a holding potential causing half-maximal current in a concentration-dependent manner, whereas it markedly enhanced sodium current of $Na_v1.8$ at a holding potential causing maximal current. Half-maximal inhibitory concentration values for $Na_v1.2$, $Na_v1.6$, and $Na_v1.7$ were 12 ± 4 (n = 6), 41 ± 2 (n = 7), and 131 ± 15 (n = 5) μmol/l (mean ± SEM), respectively. The effects of PAS were lower than those of APAS. From gating analysis, two compounds increased inactivation of all α subunits, while they showed different actions on activation of each α subunit. Moreover, two compounds showed a use-dependent block on $Na_v1.2$, $Na_v1.6$, and $Na_v1.7$.

Conclusion: APAS and PAS have diverse effects on sodium currents in oocytes expressing four α subunits. APAS inhibited the sodium currents of $Na_v1.2$ most strongly. **(ANESTHESIOLOGY 2014; 121:620-31)**

NEUROSTEROIDS are neuroactive steroids synthesized from cholesterol in both central and peripheral nervous systems, and they accumulate in the nervous system.[1] They rapidly alter neuronal excitability by mediating actions through ion-gated neurotransmitter receptors, but not through classic steroid hormone nuclear receptors.[2] Many of them are converted to sulfated metabolites by hydroxysteroid sulfotransferases, and neurosteroid sulfates are also known to regulate physiological processes. They are thought to be potentially therapeutic because of their many pharmacological properties.[3,4]

Two 3α-hydroxylated metabolites of progesterone, allopregnanolone (3α-hydroxy-5α-pregnane-20-one) and pregnanolone (3α-hydroxy-5β-pregnane-20-one), are known to be positive modulators at γ-aminobutyric acid type A ($GABA_A$) receptors with high potency.[5] These neurosteroids have been shown to have greater anesthetic potencies than those of other intravenous anesthetics that are clinically used, and not to cause acute tolerance that are observed in other

What We Already Know about This Topic

- Sodium channels are important targets for analgesic actions in the spinal cord, but their role in neurosteroid analgesia is unclear
- The effects of two sulfated neurosteroids with analgesic and anesthetic properties were tested on heterologously expressed rat voltage-gated sodium channel function

What This Article Tells Us That Is New

- The neurosteroids tested produced voltage and use-dependent block of all the subtypes tested, with more potent effects on $Na_v1.2$
- Inhibition of $Na_v1.2$ in the spinal cord by allopregnanolone is a plausible mechanism for its analgesic effects if confirmed in neuronal preparations and pain models

Submitted for publication October 25, 2013. Accepted for publication April 9, 2014. From the Department of Anesthesiology (T.H., D.O., T.M., T.K., T.S.) and Department of Pharmacology (N.Y.), School of Medicine, University of Occupational and Environmental Health, Kitakyushu, Japan; Department of Occupational Toxicology, Institute of Industrial Ecological Sciences, University of Occupational and Environmental Health, Kitakyushu, Japan (S.U.); Department of Molecular Pathology and Metabolic Disease, Faculty of Pharmaceutical Sciences, Tokyo University of Science, Chiba, Japan (Y.S.); and Cancer Pathophysiology Division, National Cancer Center Research Institute, Tokyo, Japan (Y.U.).

 Anesthesiology 2014; 121:620-31

anesthetics, suggesting usefulness of these neurosteroids as general anesthetics.[6,7] On the contrary, allopregnanolone was shown to have the most potent analgesic effects among all neurosteroids in pain models.[8] Recent studies demonstrated its analgesic effects in neuropathic pain models. Allopregnanolone alleviates thermal and mechanical hyperalgesia by ligation of the sciatic nerve in rats,[9] produces analgesic effects on formalin-induced pain in rats,[10] and prevents anticancer drug oxaliplatin-induced cold and mechanical allodynia and hyperalgesia.[11] In addition, it was suggested that stimulation of allopregnanolone synthesis might be involved in the antinociceptive effects of several analgesic drugs in neuropathic pain models.[12–14] Its effect on $GABA_A$ receptors may be important for its antinociceptive properties because GABA is involved in pain pathways in the nervous systems, and drugs targeting subtypes of GABA receptors have analgesic effects in chronic pain.[15] However, these two neurosteroids, allopregnanolone and pregnanolone, also act on other ion channels in pain signaling pathways, including T-type calcium channels[16] and *N*-methyl-D-aspartate receptors.[17]

Voltage-gated sodium channels (Na_v) have an important role in action potential initiation and propagation in excitable nerve and muscle cells. Nine α subunits ($Na_v1.1$ to $Na_v1.9$) and four auxiliary β subunits have been identified in mammals.[18,19] Each pore-forming α subunit has a different pattern of development and localization and has distinct physiological and pathophysiological roles. Sodium channel α subunits expressed in the dorsal root ganglion are considered possible targets for analgesics for inflammatory and neuropathic pain.[20–22] However, there has been little investigation on the effects of allopregnanolone on sodium channel function. It is important to examine these effects because they may be useful in clarifying the mechanisms of the analgesic effects of allopregnanolone and developing natural and safe neurosteroid-based analgesics for refractory pain. In addition, our recent report demonstrated the importance of neurosteroid sulfonation for regulation of ion channels because of more potent effects of sulfated steroid than those of nonsulfated steroids.[23] Here, we investigate the effects of two sulfated neurosteroids, allopregnanolone sulfate (APAS) and pregnanolone sulfate (PAS) (fig. 1), on several sodium channel α subunits, including $Na_v1.2$, which is expressed in the central nervous system; $Na_v1.6$, which is expressed in the central nervous system and dorsal root ganglion neurons; and $Na_v1.7$ and $Na_v1.8$, which are expressed in dorsal root ganglion neurons.

Materials and Methods

This study was approved by the Animal Research Committee of the University of Occupational and Environmental Health, Kitakyushu, Japan.

Drugs

Allopregnanolone sulfate and PAS were purchased from Steraloids, Inc. (Newport, RI).

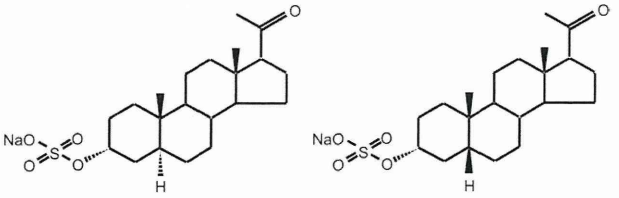

Allopregnanolone sulfate (APAS) Pregnanolone sulfate (PAS)

Fig. 1. Structures of allopregnanolone sulfate (APAS) and pregnanolone sulfate (PAS).

Plasmids

Rat $Na_v1.2$ α subunit complementary DNA (cDNA) was a gift from Dr. William A. Catterall, Ph.D. (Professor, Department of Pharmacology, University of Washington, Seattle, Washington). Rat $Na_v1.6$ α subunit cDNA was a gift from Dr. Alan L. Goldin, M.D., Ph.D. (Professor, Department of Anatomy and Neurobiology, University of California, Irvine, California). Rat $Na_v1.7$ α subunit cDNA was a gift from Gail Mandel, Ph.D. (Professor, Department of Biochemistry and Molecular Biology, Oregon Health and Science University, Portland, Oregon). Rat $Na_v1.8$ α subunit cDNA was a gift from Dr. Armen N. Akopian, Ph.D. (Assistant Professor, University of Texas Health Science Center, San Antonio, Texas), and human β_1 subunit cDNA was a gift from Dr. Alfred L. George, Jr., M.D. (Professor, Department of Pharmacology, Vanderbilt University, Nashville, Tennessee). The percentages of homology between rat and human protein of $Na_v1.2$, $Na_v1.6$, $Na_v1.7$, and $Na_v1.8$ are 98, 99, 93, and 83%, respectively, suggesting the possible limitations imposed by using rat α subunit for only $Na_v1.8$ to make conclusions in humans.

Complementary RNA (cRNA) Preparation and Oocyte Injection

After linearization of cDNA with *Cla*I ($Na_v1.2$ α subunit), *Not*I ($Na_v1.6$, 1.7 α subunits), *Xba*I ($Na_v1.8$ α subunit), and *EcoR*I (β_1 subunit), cRNAs were transcribed using SP6 (Na_v 1.8 α, β_1 subunits) or T7 ($Na_v1.2$, 1.6, and 1.7 α subunits) RNA polymerase from the mMESSAGE mMACHINE kit (Ambion, Austin, TX). Adult female *Xenopus laevis* frogs were obtained from Kyudo Co., Ltd. (Saga, Japan). *X. laevis* oocytes and cRNA microinjection were prepared as described previously.[24] Na_v α subunit cRNAs were coinjected with β_1 subunit cRNA at a ratio of 1:10 (total volume was 20 to 40 ng/50 nl) into *Xenopus* oocytes (all α subunits were coinjected with the β_1 subunit) that were randomly assigned to four α subunit groups for injection. Injected oocytes were incubated at 19°C in incubation medium, and 2 to 6 days after injection, the cells were used for electrophysiological recordings.

Electrophysiological Recordings

All electrical recordings were performed at room temperature (23°C). Oocytes were placed in a 100-μl recording chamber

and perfused at 2 ml/min with Frog Ringer's solution containing 115 mmol/l NaCl, 2.5 mmol/l KCl, 10 mmol/l HEPES, 1.8 mmol/l $CaCl_2$, pH 7.2, using a peristaltic pump (World Precision Instruments Inc., Sarasota, FL). Recording electrodes were prepared, and the whole-cell voltage clamp and recordings were achieved as described previously.[24] Transients and leak currents were subtracted using the P/N procedure, in which N subsweeps each 1/Nth of the amplitude of the main stimulus waveform (P) are applied. APAS and PAS stocks were prepared in dimethylsulfoxide and diluted in Frog Ringer's solution to a final dimethylsulfoxide concentration not exceeding 0.05%. APAS and PAS were perfused for 3 min to reach equilibrium. All recordings were performed by the experimenters who were blind to the type of compound.

The voltage dependence of activation was determined using 50-ms depolarizing pulses from a holding potential causing maximal current (V_{max}) (−90 mV for $Na_v1.2$ and $Na_v1.6$, −100 mV for $Na_v1.7$ and $Na_v1.8$) and from a holding potential causing half-maximal current ($V_{1/2}$) (from approximately −40 mV to −70 mV) to 60 mV in 10-mV increments. V_{max} and $V_{1/2}$ holding potentials induce resting and inactivated states of sodium channels. Because the effects of many analgesics in the inactivated state are known to be important for analgesic action,[25] we used these two different holding potentials to compare the effects of compounds in the resting and inactivated states. Normalized activation curves were fitted to the Boltzmann equation as described previously[24]: briefly, $G/G_{max} = 1/(1 + \exp(V_{1/2} - V)/k)$, where G is the voltage-dependent sodium conductance, G_{max} is the maximal sodium conductance, G/G_{max} is the normalized fractional conductance, $V_{1/2}$ is the potential at which activation is half maximal, and k is the slope factor. To measure steady-state inactivation, currents were elicited by a 50-ms test pulse to −20 mV for $Na_v1.2$ and $Na_v1.6$, −10 mV for $Na_v1.7$, and +10 mV for $Na_v1.8$ after 200 ms (500 ms for only $Na_v1.8$) prepulses ranging from −140 to 0 mV in 10-mV increments from a holding potential of V_{max}. Steady-state inactivation curves were fitted to the Boltzmann equation: $I/I_{max} = 1/(1 + \exp(V_{1/2} - V)/k)$, where I_{max} is the maximal sodium current, I/I_{max} is the normalized current, $V_{1/2}$ is the voltage of half-maximal inactivation, and k is the slope factor. To investigate a use-dependent sodium channel block, currents were elicited at 10 Hz by a 20-ms depolarizing pulse of −20 mV for $Na_v1.2$ and $Na_v1.6$, −10 mV for $Na_v1.7$, and +10 mV for $Na_v1.8$ from a $V_{1/2}$ holding potential in both the absence and presence of 100 μmol/l APAS and PAS. Peak currents were measured and normalized to the first pulse and plotted against the pulse number. Data were fitted to the monoexponential equation $I_{Na} = \exp(-\tau_{use} \cdot n) + C$, where n is pulse number, C is the plateau I_{Na}, and τ_{use} is the time constant of use-dependent decay.

Statistical Analysis

The GraphPad Prism software (GraphPad Software, Inc., San Diego, CA) was used to perform the statistical analysis, and a statistical power analysis was performed using G*Power software. All values are presented as means ± SEM. The n values refer to the number of oocytes examined. Each experiment was performed with oocytes taken from at least two frogs. Data were statistically evaluated by paired t test (two-tailed). We assessed the inhibitory effects at different APAS concentrations in the concentration–response curve, using one-way ANOVA followed by Dunnet *post hoc* test for multiple comparisons. Hill slope, half-maximal inhibitory concentration (IC_{50}), and half-maximal effective concentration

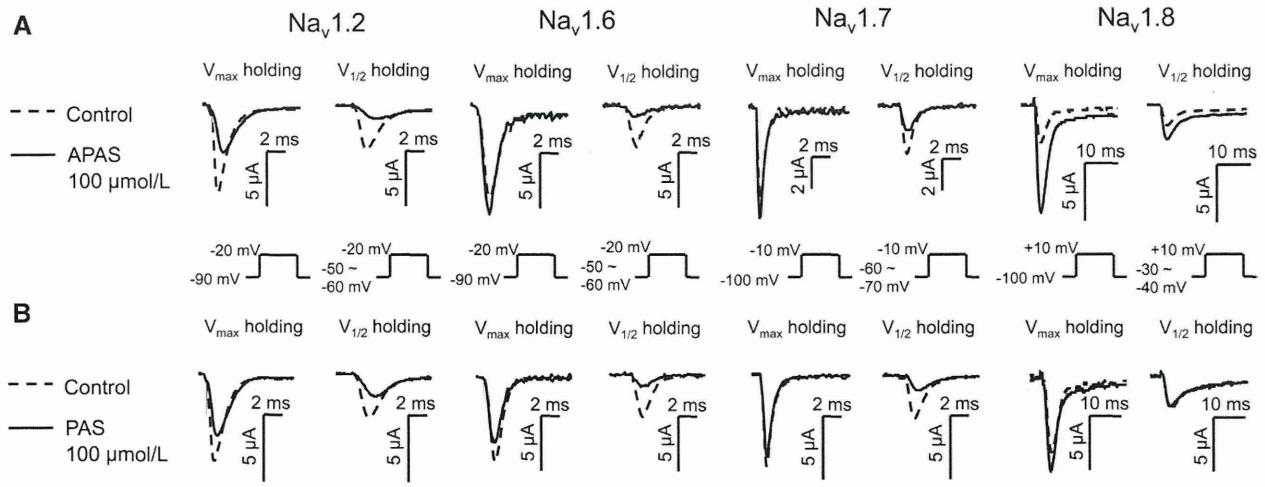

Fig. 2. Effects of allopregnanolone sulfate (APAS) (*A*) and pregnanolone sulfate (PAS) (*B*) on peak sodium inward currents in *Xenopus* oocytes expressing $Na_v1.2$, $Na_v1.6$, $Na_v1.7$, or $Na_v1.8$ α subunits with β_1 subunits at two holding potentials. Representative traces are shown. Sodium currents were evoked by 50-ms depolarizing pulses to −20 mV for $Na_v1.2$ and $Na_v1.6$, −10 mV for $Na_v1.7$, and +10 mV for $Na_v1.8$ from V_{max} or $V_{1/2}$ in both the absence and presence of 100 μmol/l of the compounds. Na_v = voltage-gated sodium channel; V_{max} holding = holding potential causing maximal current; $V_{1/2}$ holding = holding potential causing half-maximal current.

(EC_{50}) values were also calculated. *P* value less than 0.05 was considered to indicate a significant difference.

Results

Effects of APAS and PAS on Peak Na^+ Inward Currents Elicited from Two Different Holding Potentials

Currents were elicited using a 50-ms depolarizing pulse to −20 mV for $Na_v1.2$ and $Na_v1.6$, −10 mV for $Na_v1.7$, and +10 mV for $Na_v1.8$ applied every 10 s from a V_{max} or $V_{1/2}$ holding potential in both the absence and presence of 100 μmol/l APAS and PAS (fig. 2). The amplitude of expressed sodium currents was typically 2 to 15 μA, and oocytes that showed a maximal current greater than 20 μA were not included in the data collection in all the following experiments. APAS had dual effects on sodium currents depending on the holding potential and α subunit (figs. 2 and 3). At $V_{1/2}$, APAS reduced the peak I_{Na} (sodium current) induced by $Na_v1.2$, $Na_v1.6$, and $Na_v1.7$ by 79 ± 1%, 71 ± 2%, and 49 ± 3%, respectively. At V_{max}, APAS also reduced I_{Na} induced by $Na_v1.2$ by 60 ± 4%, whereas it enhanced I_{Na} induced by $Na_v1.6$ and $Na_v1.7$ by 15 ± 6% and 14 ± 1%, respectively, although these effects were small. In contrast, APAS greatly enhanced I_{Na} induced by $Na_v1.8$ at both $V_{1/2}$ and V_{max} by 112 ± 34% and 202 ± 14%, respectively (fig. 3A). PAS reduced I_{Na} induced by $Na_v1.2$, $Na_v1.6$, and $Na_v1.7$ at $V_{1/2}$ by 54 ± 4%, 71 ± 1%, and 48 ± 2%, respectively. Effects of PAS on I_{Na} at V_{max} were smaller than those at $V_{1/2}$, and the magnitudes of inhibitory effects on $Na_v1.2$, $Na_v1.6$, and $Na_v1.7$ were 31 ± 5%, 10 ± 1%, and 6 ± 1%, respectively. While PAS enhanced I_{Na} induced by $Na_v1.8$ at V_{max} by 39 ± 6%, it did not affect I_{Na} induced by $Na_v1.8$ at $V_{1/2}$ (fig. 3B). In summary, PAS inhibited I_{Na} induced by $Na_v1.2$, $Na_v1.6$, and $Na_v1.7$ at both $V_{1/2}$ and V_{max} holding potentials. APAS had inverse effects on $Na_v1.6$ and $Na_v1.7$ according to the different holding potentials, whereas it suppressed I_{Na} induced by $Na_v1.2$ at both $V_{1/2}$ and V_{max}. Moreover, APAS markedly enhanced I_{Na} induced by $Na_v1.8$ at both $V_{1/2}$ and V_{max}.

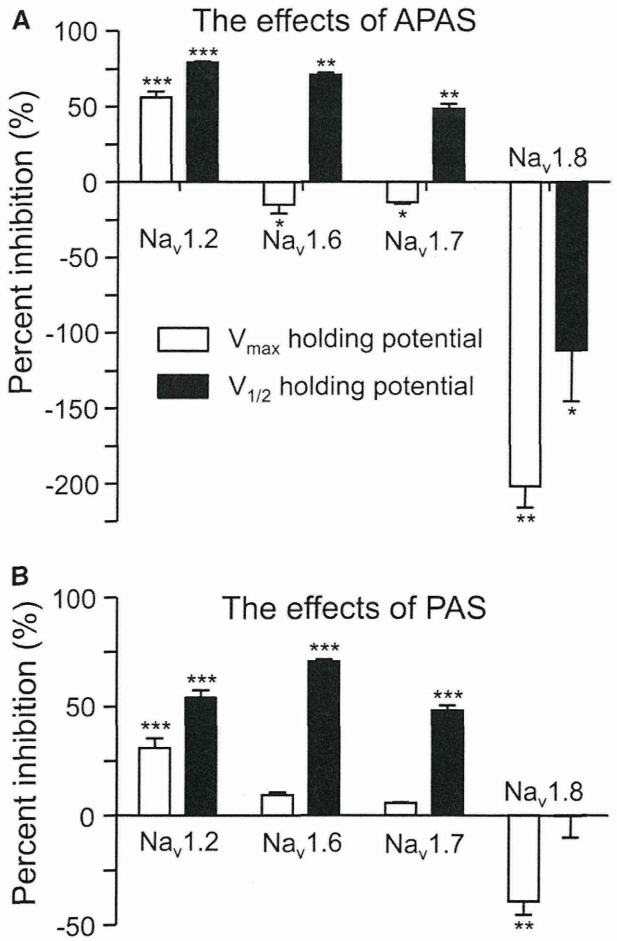

Fig. 3. Percentage inhibition of sodium currents of allopregnanolone sulfate (APAS) (n = 6) (*A*) and pregnanolone sulfate (PAS) (n = 5) (*B*) were calculated. *Open columns* represent the effect at V_{max} holding potential, and *closed columns* indicate the effect at $V_{1/2}$. Data are presented as means ± SEM. **P* < 0.05, ***P* < 0.01, and ****P* < 0.001 compared with the control, based on paired *t* test (two-tailed). Na_v = voltage-gated sodium channel; V_{max} holding potential = holding potential causing maximal current; $V_{1/2}$ holding potential = holding potential causing half-maximal current.

Next, we examined the concentration–response relationship for suppression of the peak I_{Na} induced through $Na_v1.2$, $Na_v1.6$, and $Na_v1.7$ by APAS and PAS at $V_{1/2}$ holding potential because suppression by both neurosteroids of these α subunits at $V_{1/2}$ was more potent than that at V_{max} (fig. 4, A and B). In addition, we investigated the concentration–response relationship for potentiation of the peak I_{Na} of $Na_v1.8$ by APAS and PAS at V_{max}, because both neurosteroids showed potent enhancement of I_{Na} at V_{max} compared with that at $V_{1/2}$ (fig. 4C). IC_{50} values, EC_{50} values, and Hill slopes calculated from nonlinear regression analyses of the dose–response curves are shown in table 1. From these analyses, the effect of APAS on $Na_v1.2$ was the most potent among the two neurosteroids and four α subunits.

Effects of APAS and PAS on Activation of Sodium Currents

We examined the effects of APAS and PAS on four α subunits in sodium current activation. Voltage dependence of activation was determined using 50-ms depolarizing pulses from a holding potential of V_{max} to 50 mV in 10-mV increments or from a holding potential of $V_{1/2}$ to 60 mV in 10-mV increments for $Na_v1.2$, $Na_v1.6$, $Na_v1.7$, and $Na_v1.8$ in both the absence and presence of 100 μmol/l APAS and PAS (fig. 5). Activation curves were derived from the I–V curves (see Electrophysiological Recordings under Materials and Methods). At V_{max}, APAS greatly reduced the peak I_{Na} induced by $Na_v1.2$, whereas it greatly enhanced the peak I_{Na} induced by $Na_v1.8$ in the depolarizing region where channel opening begins. It also enhanced the peak I_{Na} induced by $Na_v1.6$ and $Na_v1.7$, similar to its effects on $Na_v1.8$, although both effects were small. At $V_{1/2}$, APAS greatly suppressed the peak I_{Na} induced by $Na_v1.2$, $Na_v1.6$, and $Na_v1.7$,

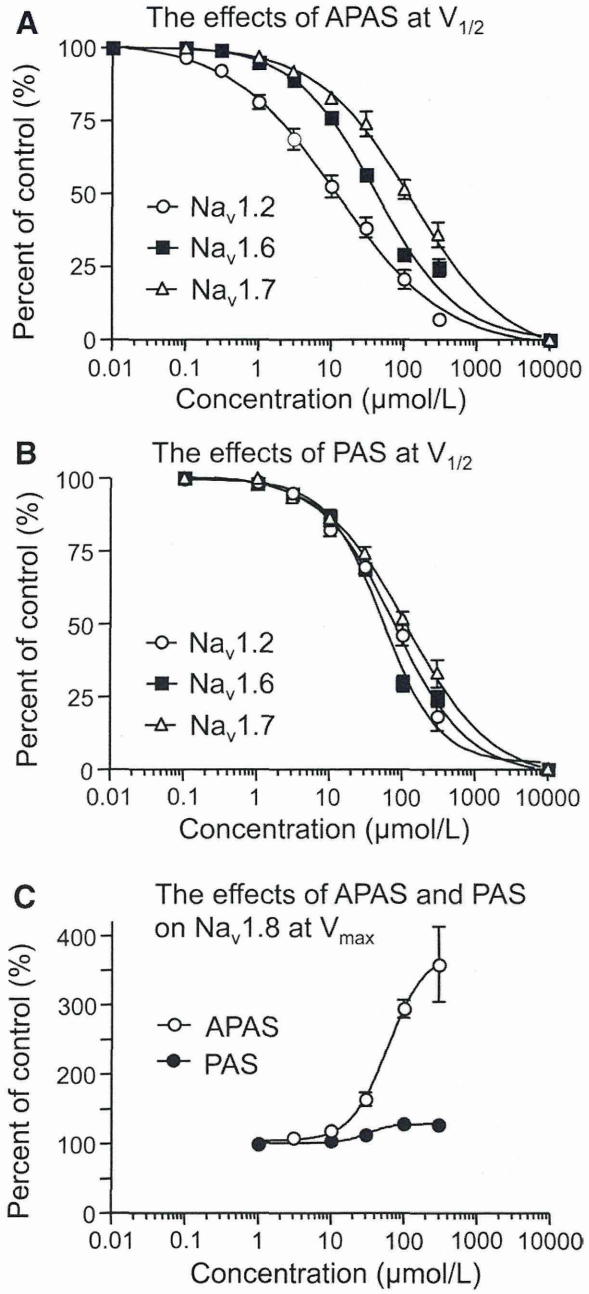

Fig. 4. Concentration–response curves for two-compound suppression of sodium currents elicited by 50-ms depolarizing pulses to −20 mV for $Na_v1.2$ (n = 6) and $Na_v1.6$ (n = 7) and −10 mV for $Na_v1.7$ (n = 5) from $V_{1/2}$ holding potential (*A* and *B*) and those for two-compound potentiation of sodium currents elicited by 50-ms depolarizing pulses to +10 mV for $Na_v1.8$ (n = 5) from V_{max} (*C*). The peak current amplitude in the presence of two compounds was normalized to that of the control, and the effects are expressed as percentages of the control. Hill slopes, IC_{50} values, and EC_{50} values are shown in table 1. Data are presented as means ± SEM. Data were fitted to the Hill slope equation to give the Hill slopes, IC_{50} values, and EC_{50} values. Hill slopes, IC_{50} values, and EC_{50} values were calculated using GraphPad Prism (GraphPad Software, Inc., San Diego, CA). APAS = allopregnanolone sulfate; Na_v = voltage-gated sodium channel; PAS = pregnanolone sulfate; V_{max} = holding potential causing maximal current; $V_{1/2}$ = holding potential causing half-maximal current.

but it enhanced the peak I_{Na} induced by $Na_v1.8$, similar to its effects on $Na_v1.8$ at V_{max}. PAS reduced I_{Na} induced by $Na_v1.2$, $Na_v1.6$, and $Na_v1.7$ at both $V_{1/2}$ and V_{max}, whereas it enhanced I_{Na} induced by $Na_v1.8$ in the depolarizing region at V_{max}, but had no effect at $V_{1/2}$.

At V_{max} holding potential, APAS significantly shifted the midpoint of the steady-state activation ($V_{1/2}$) in a depolarizing direction for $Na_v1.2$, but it significantly shifted $V_{1/2}$ in a hyperpolarizing direction for $Na_v1.6$, $Na_v1.7$, and $Na_v1.8$. At $V_{1/2}$, APAS also shifted $V_{1/2}$ in a similar direction as the shift at V_{max}, although the shift was small and not significant, except for $Na_v1.8$. The shifts of $V_{1/2}$ by PAS were smaller than those by APAS. PAS significantly shifted $V_{1/2}$ in a depolarizing direction for $Na_v1.2$ and $Na_v1.6$ at $V_{1/2}$, but it had no or slight effects on all α subunits at V_{max}, and on $Na_v1.7$ and $Na_v1.8$ at $V_{1/2}$ (fig. 6 and tables 2 and 3).

Effects of APAS and PAS on Inactivation of Sodium Currents

We also investigated the effects of APAS and PAS on steady-state inactivation. Currents were elicited by a 50-ms test pulse to −20 mV for $Na_v1.2$ and $Na_v1.6$, −10 mV for $Na_v1.7$, and +10 mV for $Na_v1.8$ after 200 ms (500 ms for only $Na_v1.8$) prepulses ranging from −140 mV to 0 mV in 10-mV increments from V_{max} holding potential. Steady-state inactivation curves were fitted to the Boltzmann equation (see Electrophysiological Recordings under Materials and Methods). APAS and PAS significantly shifted the midpoint of steady-state inactivation ($V_{1/2}$) in the hyperpolarizing direction for all α subunits; APAS shifted by 8.0, 8.9, 6.7, and 8.9 mV and PAS shifted by 4.5, 8.0, 6.6, and 10.2 mV for $Na_v1.2$, $Na_v1.6$, $Na_v1.7$, and $Na_v1.8$, respectively (fig. 7 and tables 2 and 3). The effects of APAS and PAS in the hyperpolarizing range were consistent with the effects of these two neurosteroids on the peak I_{Na} at V_{max} and their effects on the I–V curves in the hyperpolarizing range at V_{max}.

Use-dependent Block of Sodium Currents by APAS and PAS

The use-dependent block of sodium currents by APAS and PAS was also investigated. Currents were elicited at 10 Hz by a 20-ms depolarizing pulse of −20 mV for $Na_v1.2$ and $Na_v1.6$ and −10 mV for $Na_v1.7$ from a $V_{1/2}$ holding potential in both the absence and presence of 100 μmol/l APAS and PAS. Peak currents were measured and normalized to the first pulse and plotted against the pulse number (fig. 8, A–D). Data were fitted by the monoexponential equation (see Electrophysiological Recordings under Materials and Methods). APAS significantly reduced the plateau I_{Na} amplitude of $Na_v1.2$, $Na_v1.6$, and $Na_v1.7$ from 0.80 ± 0.03 to 0.57 ± 0.03, 0.89 ± 0.01 to 0.49 ± 0.07, and 0.89 ± 0.02 to 0.62 ± 0.06, respectively (fig. 8E). PAS also reduced the plateau I_{Na} amplitudes of $Na_v1.2$, $Na_v1.6$, and $Na_v1.7$ from 0.81 ± 0.2 to 0.70 ± 0.03, 0.94 ± 0.01 to 0.73 ± 0.02, and 0.91 ± 0.02 to 0.75 ± 0.01, respectively, and the reductions

Table 1. Fitted Parameters for Effects of APAS and PAS

	APAS			PAS		
	IC_{50}	EC_{50}	Hill Slope	IC_{50}	EC_{50}	Hill Slope
$Na_v1.2$	12.2 ± 3.5		0.58 ± 0.07	78.4 ± 9.8		0.86 ± 0.03
$Na_v1.6$	40.6 ± 1.9		0.77 ± 0.03	53.8 ± 3.2		1.12 ± 0.03
$Na_v1.7$	130.7 ± 14.7		0.67 ± 0.06	117.8 ± 19.0		0.74 ± 0.04
$Na_v1.8$		61.3 ± 8.5	1.72 ± 0.10		32.7 ± 3.4	2.45 ± 0.47

IC_{50} values, EC_{50} values, and Hill slopes calculated from nonlinear regression analyses of the dose–response curves shown in figure 4. Data are given as mean ± SEM; n = 6 ($Na_v1.2$), 7 ($Na_v1.6$), 5 ($Na_v1.7$), and 5 ($Na_v1.8$).

APAS = allopregnanolone sulfate; EC_{50} = half-maximal effective concentration; IC_{50} = half-maximal inhibitory concentration; Na_v = voltage-gated sodium channel; PAS = pregnanolone sulfate.

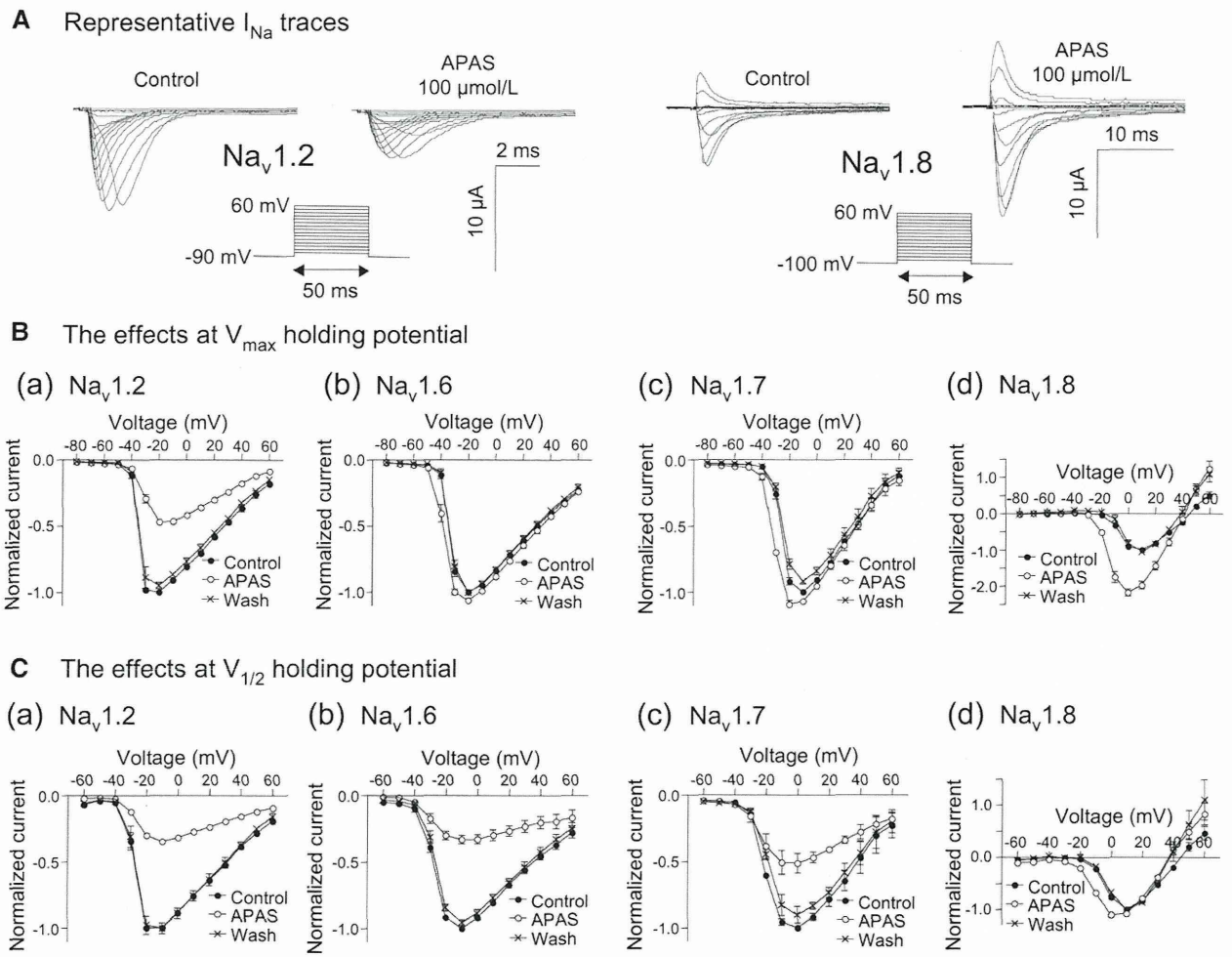

Fig. 5. Effects of allopregnanolone sulfate (APAS) on I–V curves of sodium currents in oocytes expressing $Na_v1.2$ (*a*) (n = 5), $Na_v1.6$ (*b*) (n = 7), $Na_v1.7$ (*c*) (n = 5), or $Na_v1.8$ (*d*) (n = 6) α subunits with β_1 subunits. Currents were elicited using 50-ms depolarizing steps between −80 and 60 mV in 10-mV increments from a V_{max} holding potential and elicited using 50-ms depolarizing steps between −60 and 60 mV in 10-mV increments from a $V_{1/2}$ holding potential. (*A*) Representative I_{Na} traces from oocytes expressing $Na_v1.2$ (*left*) and $Na_v1.8$ (*right*) with the β_1 subunit in both the absence and presence of 100 µmol/l of APAS at V_{max} holding potential are shown. The effects of APAS on normalized I–V curves elicited from V_{max} (*B*) and $V_{1/2}$ holding potentials (*C*) are shown (*closed circles*, control; *open circles*, neurosteroids; *cross*, washout). Peak currents were normalized to the maximal currents observed from −20 to +10 mV. Data are presented as means ± SEM. Na_v = voltage-gated sodium channel; V_{max} holding potential = holding potential causing maximal current; $V_{1/2}$ holding potential = holding potential causing half-maximal current; Wash = washout.

were significant except for $Na_v1.2$ (fig. 8F). These results demonstrated a use-dependent block of APAS and PAS on sodium channels, and the block by APAS was more potent than that by PAS.

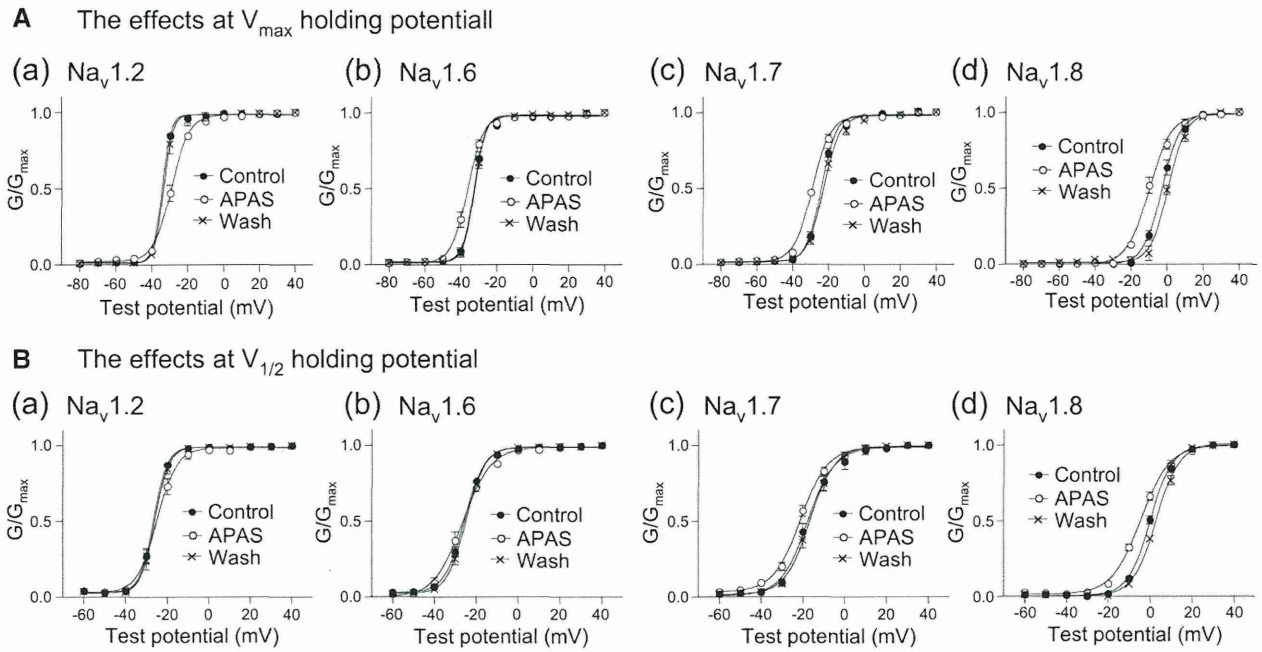

Fig. 6. Effects of allopregnanolone sulfate (APAS) on channel activation in oocytes expressing $Na_v1.2$ (*a*) (n = 5), $Na_v1.6$ (*b*) (n = 7), $Na_v1.7$ (*c*) (n = 5), or $Na_v1.8$ (*d*) (n = 6) α subunits with β_1 subunits from V_{max} (*A*) or $V_{1/2}$ holding potentials (*B*). *Closed circles*, *open circles*, and *cross* represent control, the effect of neurosteroids, and washout, respectively. Data are expressed as means ± SEM. Activation curves were fitted to the Boltzmann equation; $V_{1/2}$ is shown in table 2. Na_v = voltage-gated sodium channel; V_{max} holding potential = holding potential causing maximal current; $V_{1/2}$ holding potential = holding potential causing half-maximal current; Wash = washout.

Table 2. Effects of APAS on Activation and Inactivation

	$V_{1/2}$ (mV)					
	Holding V_{max}			Holding $V_{1/2}$		
	Control	APAS	Shift	Control	APAS	Shift
Activation						
$Na_v1.2$	−34.2±0.5	−29.1±1.0**	+5.1	−26.4±0.8	−24.8±1.1	+1.6
$Na_v1.6$	−32.5±0.6	−36.3±0.9***	−3.8	−25.6±0.6	−26.7±1.3	−1.1
$Na_v1.7$	−23.9±0.6	−29.0±0.3***	−5.1	−17.2±1.7	−20.9±0.9	−3.7
$Na_v1.8$	−2.7±1.1	−9.8±1.2***	−7.1	0.3±0.6	−4.2±0.8**	−4.5
Inactivation						
$Na_v1.2$	−50.1±1.0	−58.1±1.1***	−8.0			
$Na_v1.6$	−57.8±0.5	−66.7±0.7***	−8.9			
$Na_v1.7$	−72.3±1.6	−79.0±1.8***	−6.7			
$Na_v1.8$	−37.0±2.2	−45.9±1.7***	−8.9			

$V_{1/2}$ is calculated from nonlinear regression analyses of activation and inactivation curves shown in figures 6 and 7. Data are given as mean ± SEM; n = 5 ($Na_v1.2$), 7 ($Na_v1.6$), 5 ($Na_v1.7$), and 6 ($Na_v1.8$).

**$P < 0.01$; ***$P < 0.001$ compared with control, based on paired *t* test (two-tailed).

APAS = allopregnanolone sulfate; Holding V_{max} = holding potential causing maximal current; Holding $V_{1/2}$ = holding potential causing half-maximal current; Na_v = voltage-gated sodium channel; $V_{1/2}$ = the potential at which activation is half maximal for activation curve, and the voltage of half-maximal inactivation for inactivation curve.

Discussion

In the current study, we demonstrated that APAS and PAS differentially affected I_{Na} induced by four α subunits at both V_{max} and $V_{1/2}$ holding potentials. Moreover, we found that both neurosteroids suppress $Na_v1.2$, $Na_v1.6$, and $Na_v1.7$ at $V_{1/2}$ in a concentration-dependent manner. IC_{50} values indicated that the effect of APAS on $Na_v1.2$ was most potent among the two compounds and three α subunits. To the best of our knowledge, this is the first direct evidence of the various effects of these two neurosteroids on neuronal sodium channel α subunits. It is thought that APAS is synthesized from allopregnanolone by 3α-hydroxysteroid

Table 3. Effects of PAS on Activation and Inactivation

	$V_{1/2}$ (mV)					
	Holding V_{max}			Holding $V_{1/2}$		
	Control	PAS	Shift	Control	PAS	Shift
Activation						
$Na_v1.2$	−33.4 ± 0.6	−30.5 ± 1.5	+2.9	−26.1 ± 0.9	−23.7 ± 1.1**	+2.4
$Na_v1.6$	−32.1 ± 0.5	−32.4 ± 0.8	−0.3	−24.8 ± 0.8	−20.7 ± 1.4**	+4.1
$Na_v1.7$	−23.2 ± 0.5	−23.9 ± 0.6	−0.7	−18.7 ± 1.0	−18.0 ± 0.9	+0.7
$Na_v1.8$	−1.4 ± 2.1	−2.3 ± 1.7	−0.9	−0.2 ± 0.8	−1.1 ± 0.9	−0.9
Inactivation						
$Na_v1.2$	−49.9 ± 0.8	−54.4 ± 1.5**	−4.5			
$Na_v1.6$	−57.5 ± 0.5	−65.5 ± 0.5***	−8.0			
$Na_v1.7$	−72.3 ± 1.0	−78.9 ± 1.0***	−6.6			
$Na_v1.8$	−36.0 ± 1.3	−46.2 ± 1.4**	−10.2			

$V_{1/2}$ is calculated from nonlinear regression analyses of activation and inactivation curves (not shown). Data are given as mean ± SEM; n = 6 ($Na_v1.2$), 7 ($Na_v1.6$), 5 ($Na_v1.7$), and 6 ($Na_v1.8$).

** $P < 0.01$; *** $P < 0.001$ compared with control, based on paired *t* test (two-tailed).

Holding V_{max} = holding potential causing maximal current; Holding $V_{1/2}$ = holding potential causing half-maximal current; Na_v = voltage-gated sodium channel; PAS = pregnanolone sulfate; $V_{1/2}$ = the potential at which activation is half maximal for activation curve, and the voltage of half-maximal inactivation for inactivation curve.

sulfotransferase *in vivo*, because 3α-hydroxysteroid sulfotransferase has been isolated *in vivo*.[26] Therefore, allopregnanolone likely exerts a portion of its effects through APAS, which is its metabolite.

It was reported that the level of endogenous allopregnanolone changes in many physiological and pathological situations within a serum concentration range of 1 to 10 nmol/l.[27,28] However, it is not clear whether allopregnanolone has an analgesic effect in physiological concentrations. A recent study demonstrated that 1 and 10 μmol/l of allopregnanolone reduced mechanical allodynia and thermal heat hyperalgesia in normal and neuropathic pain models in rats after 10-μl intrathecal injection.[29] Another investigator reported that intrathecal administration of 10 μmol/l of allopregnanolone showed antihyperalgesic effects in hyperalgesic rats after spinal nerve ligation.[30] From these previous studies, concentrations approximately 1 μmol/l allopregnanolone at receptive fields are estimated to have an analgesic effect. In the current study, APAS tended to, *albeit* not significantly, suppress the I_{Na} of $Na_v1.2$ at 0.3 μmol/l by 8% and significantly ($P < 0.01$) inhibited it at 1 μmol/l by 19 ± 2%. The IC_{50} value of $Na_v1.2$ inhibition by APAS was 12 μmol/l. It was reported that relatively small degrees of sodium channel inhibition could have profound effects on the neuronal firing rate because a 10% inhibition of sodium current reduces the number of action potentials to 10 from a control response of 21 in 750 ms.[24] Therefore, APAS may reduce neuronal firing for $Na_v1.2$ at a concentration exhibiting the antinociceptive effects of allopregnanolone in animal models, whereas the effects of APAS and PAS on another three α and four α subunits, respectively, may not be pharmacologically relevant because these effects were observed at concentrations over 10 μmol/l. In addition, the effects of highly hydrophobic compounds—such as neurosteroids—we used tend to be attenuated in the voltage-clamp techniques with *Xenopus* oocytes, compared with the whole-cell voltage-clamp methods using mammalian cells. Indeed, it was reported that the enhancing effect by allopregnanolone on $GABA_A$ receptor combination ($\alpha_1\beta_2\gamma_{2L}$) was more potent in the human embryonic kidney 293 cells system (EC_{50}; 41 ± 2 nmol/l)[31] than that in the *Xenopus* oocyte system (EC_{50}; 177 ± 2 nmol/l).[32] This may be a limitation of experiments using the *Xenopus* oocyte expression system; this limitation indicates that APAS might inhibit function of $Na_v1.2$ more potently in a mammalian cell system than in the oocyte system, however, it also could potentiate $Na_v1.8$ function more potently in a mammalian cell. Therefore, further investigation is needed to consider the roles of these α subunits in humans.

Analysis of gating revealed common characteristics but also some differences in the effects of APAS and PAS on different α subunits. A common effect on all α subunits was enhancement of inactivation. Because of this enhancement effect, the inhibitions by two compounds at $V_{1/2}$ holding potentials could be interpreted as stronger effects because they shift inactivation curve to the hyperpolarizing direction, which makes the channel into further inactivated state. In contrast, APAS enhanced peak I_{Na} at V_{max}, shifted activation in the hyperpolarizing direction, and increased sodium currents in the hyperpolarizing range of the inactivation curves for $Na_v1.6$, $Na_v1.7$, and $Na_v1.8$. These changes indicate that APAS shifts channel gating equilibrium toward the open channel state and activates sodium channels. This action might attenuate the effects on the inactivated state and, especially, lead to enhancement of I_{Na} even in the inactivated state ($V_{1/2}$ holding potential) for $Na_v1.8$ in spite of the great enhancement of inactivation. However, for $Na_v1.2$, APAS profoundly suppressed peak I_{Na} at V_{max}, shifted activation in the depolarizing direction at V_{max}, and greatly decreased